Available online at www.sciencedirect.com
SCIENCE DIRECT
Forest Ecology and Management 224 (2006) 104–118
Forest Ecology and Management
www.elsevier.com/locate/foreco

Effective slope lengths for buffering hillslope surface runoff in fragmented landscapes in northern Vietnam

Alan D. Ziegler [a,*], Liem T. Tran [b], Thomas W. Giambelluca [a], Roy C. Sidle [c], Ross A. Sutherland [a], Michael A. Nullet [a], Tran Duc Vien [d]

[a] *Geography Department, University of Hawaii, 2424 Maile Way Saunders Hall 445, Honolulu, HI 96822, USA*
[b] *Department of Geography & Geology, Florida Atlantic University, Boca Raton, FL, USA*
[c] *Disaster Prevention Research Institute, Geohazards Division, Kyoto University, Kyoto, Japan*
[d] *Center for Natural Resources and Environmental Studies (CRES), Vietnam National University, Hanoi, Vietnam*

Abstract

We use field observations and diagnostic computer simulations (KINEROS2) to estimate the effective slope lengths (ESL) for buffers on disturbed hillslopes in two fragmented basins in northern Vietnam. Grassland, disturbed forest, and intermediate forms of secondary vegetation are the most effective buffering vegetation in the study area because these surfaces tend to have the highest saturated hydraulic conductivity. The ESL (m) is described by the following function of slope (m m^{-1}): ESL = 98 + 15 ln(slope). This non-linear relationship predicts comparatively longer buffer lengths at gentle slope gradients than guidelines/practices currently in use. The predicted buffer lengths range from roughly 30 to 100 m for slope gradients ranging from 0.01 to 1.0 m m^{-1}. However, for large storms, steeper slopes, and/or more degraded conditions, buffer lengths greater than those predicted by the ESL criteria may be needed to minimize impacts from overland flow. On slopes with particularly large contributing areas, multiple or staggered buffers may be required. For the occurrence of concentrated overland flow, no practical buffer length may be sufficient. The ESL estimations provide a starting point for determining appropriate buffer dimensions needed to infiltrate upslope surface runoff in disturbed montane watersheds at the study site. Final determination of buffer dimensions should consider the physical characteristics of contributing hillslopes, the nature of the material to be filtered (e.g., water, sediment, chemicals, nutrients), and the likelihood of adoption of any buffering practice. Finally, buffers should be regarded as complementary practices to other hillslope conservation activities. Recognizing that the use of long buffer lengths may not be feasible for steep terrain in intensely managed tropical watersheds, we derive a second equation to predict the minimal effective slope length (MESL) for buffers: MESL = 32 + 4 ln(slope). MESL values range from approximately 15 to 30 m over the same slope gradients, but they are less effective at reducing HOF than ESL buffers, particularly for large storms when erosion risk is highest.

Keywords: Hortonian overland flow; Vegetative buffer strips; Land degradation; Swidden agriculture; KINEROS2; Southeast Asia

1. Introduction

Forest fragmentation occurs when continuous forest tracts are converted to various replacement cover types interspersed with patches of remnant forest (Laurance and Bierregaard, 1997). Such fragmentation is common throughout current landscapes in much of Southeast Asia as well as in many areas of South America and Africa. Important hydrological processes, such as evapotranspiration and infiltration, often differ on replacement covers, compared with the undisturbed forest (Bruijnzeel, 2001; Giambelluca, 2002). In two fragmented basins near Tanh Minh Village in northern Vietnam, for example, saturated hydraulic conductivity (K_s) on most replacement land covers is less than that for forest (Ziegler et al., 2004). The landscape is therefore a mosaic of surfaces differing in the propensity to generate Hortonian overland flow (HOF, caused when rainfall rate exceeds infiltration capacity and surface storage; Horton, 1933). Because of the high degree of spatial heterogeneity in land cover, HOF generated on upslope areas of low K_s can re-infiltrate on downslope surfaces of high K_s (i.e., buffers), potentially reducing both surface erosion on the hillslope and the total depth of surface runoff that enters the stream network.

The concept of vegetation buffers in riparian corridors and lower hillslopes adjacent to streams has different meanings depending on the following: (1) the 'material' or phenomena effected (e.g., water, eroded surface sediment, landslide

* Corresponding author. Fax: +1 808 956 3512.
E-mail address: adz@hawaii.edu (A.D. Ziegler).
URL: http://webdata.soc.hawaii.edu/hydrology/

0378-1127/$ – see front matter © 2005 Elsevier B.V. All rights reserved.
doi:10.1016/j.foreco.2005.12.011

material, chemicals, nutrients, bacteria, species diversity, temperature); (2) the water body or property being protected; and (3) the inherent aquatic-terrestrial linkages (Lynch et al., 1985; Smith, 1992; Jordan et al., 1993; Barling and Moore, 1994; Castelle et al., 1994; Maag et al., 1997; Jacinthe et al., 1998; Lee et al., 2000, 2004; Gomi et al., 2002; Lowrance et al., 2002; Schultz et al., 2004). Implicit in the term buffering is a reduction in the total volume and/or peak flux of material transported during a storm event. Herein, we consider buffering to denote a reduction of the total HOF depth during discrete storm events. We recognize that the degree to which buffering of overland flow occurs on fragmented hillslopes depends, in part, on the extent to which buffers are located below HOF source areas. Importantly, the downslope vegetation must occupy a sufficient slope length to be an effective buffer.

The objective in this paper is to establish, via diagnostic overland flow simulations, the effective slope length (ESL) needed to infiltrate shallow unconcentrated HOF generated from upslope sources in Tanh Minh, Vietnam. Others may refer to ESL as the effective 'width' (e.g., in reviews by Clinnick, 1985; Norris, 1993; Barling and Moore, 1994). This objective has direct application to establishing/designing hillslope buffers for protecting water quality at the Tanh Minh study site. In a larger context, assessing the slope lengths required to infiltrate HOF generated from upslope areas is useful in improving our conceptual understanding of the degree to which various land-cover surfaces in fragmented landscapes within the region can influence hydrological response—e.g., by influencing the generation and buffering of HOF (Ziegler et al., 2004).

2. Study area

Tanh Minh (roughly 19:00N, 104:45E) is located SSW of Hanoi, in Da Bac District of Hoa Binh Province, northern Vietnam (Fig. 1). The study area is described in more detail elsewhere (Ziegler et al., 2004). Two watersheds comprise the study area (Fig. 2): Watershed 1 (WS1—910 ha) is located on the west side of the study area; the larger WS2 (1228 ha) on the east side. Elevation ranges from roughly 200 to 1000 m asl. Slopes are steep, typically 0.5–1.7 m m^{-1}; they extend to the valley floor and/or stream channel. Parent bedrock is largely sandstone and schist, with some mica-bearing granite present. Soils are predominantly ultisols of the udic moisture regime. Soil depths on hillslopes typically exceed 2 m. The climate is characterized as tropical monsoon; approximately 90% of the annual 1800 mm of rainfall occurs between May and October.

Remnant natural forest patches exist primarily on steep, relatively inaccessible peaks, ravines, and slopes. Some accessible hilltops and ridgelines do, however, host mature secondary forests (Fig. 3d). Mountain slopes are dotted with active swidden fields that are farmed by the Tay villagers, the primary inhabitants of Tanh Minh (Fig. 3e). Juxtaposed with active fields are recently abandoned fields and various stages of secondary vegetation (mixtures of grasses, herbs, bamboo, and small trees) that have emerged on formerly cultivated sites (Fig. 3b and d). Previously, eight major land-cover classes were

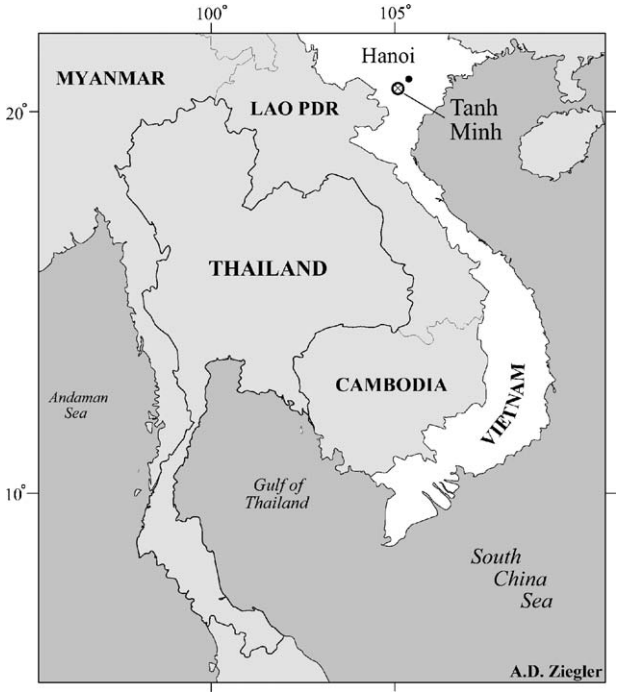

Fig. 1. The study area, Tanh Minh, in northern Vietnam.

identified: upland fields (UF), abandoned fields (AF), young secondary vegetation (YSV), grasslands (GL), intermediate secondary vegetation (ISV), forest (F), consolidated surface (CS), and paddy fields (PF) (Ziegler et al., 2004). Vegetation descriptions are listed in Appendix A.

A color map showing the land-cover distribution in Tanh Minh is available elsewhere (Ziegler et al., 2004). Land-cover areas and fragmentation-related data in Table 1 are based on analysis of a 30 m × 30 m land-cover classification and a DEM (described in Ziegler et al., 2004). Consolidated surfaces, such as paths and roads, are not included in Table 1 because they are sub-grid-cell features that collectively occupy less than 1% of the basin area. Basic soil physical properties determined on

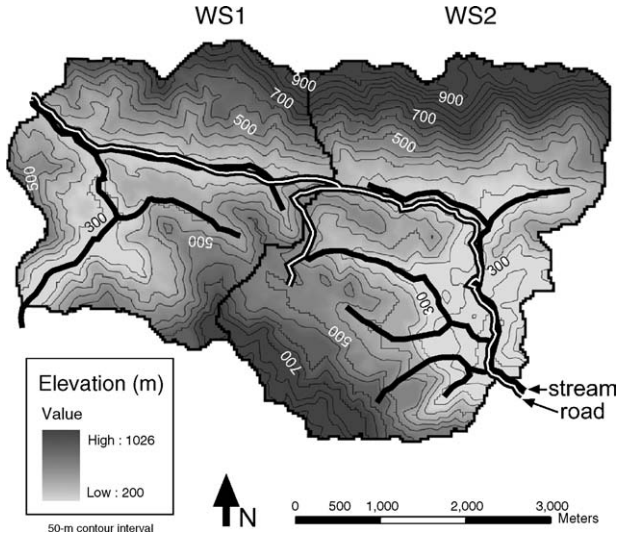

Fig. 2. Elevation map for the two principal watersheds studied; a colored land-cover map is shown in a prior work (Ziegler et al., 2004).

Fig. 3. (a) Recently abandoned field from which overland flow passes through a narrow buffer before entering an intermittent stream; (b) grassland vegetation growing on a former swidden site; (c) two newly cleared fields surrounded by young secondary vegetation, which is a generally ineffective buffering land cover; (d) a large forest fragment on the upper hillslope and ridge above swidden agriculture sites and farmer dwellings (by Steve Leisz); (e) a Tay woman, Kim, harvesting paddy rice.

hillslope land covers are listed in Table 2 (rice paddies are not listed). Collection locations and methods for these properties are described in a prior paper (Ziegler et al., 2004).

Hillslope fields (upland rice, corn, cassava) range in size from approximately 400 m^2 to >1 ha—and some cultivated hillslope gradients exceed 1 m m^{-1} (Fig. 3c). A typical cropping cycle can be described briefly as follows (Lan, a Tay villager, pers. commun.): after clearing, a field is cultivated for 2–4 years (depending on the crop yield in the final year), followed by a fallow period of at least 2 years (depending on the needs of the family). This cycle is repeated – again, with the lengths of the cropping and fallow periods determined by

Table 1
Area and fragmentation-related statistics for the two combined watersheds investigated

Land cover	ID	Total patches	Land-cover area (ha)	Relative area (%)	Mean patch area (ha)	Mean elevation (m)	Mean slope (m m^{-1})
Upland field	UF	104	326	15.2	3.1	402	0.19
Abandoned field	AF	149	330	15.4	2.2	400	0.21
Grasslands	GL	59	806	37.7	13.7	426	0.19
Young secondary vegetation	YSV	87	202	9.5	2.3	610	0.25
Intermediate secondary vegetation	ISV	53	387	18.1	7.3	677	0.29
Forest	F	29	27	1.3	0.9	359	0.19
Rice paddy	RP	50	59	2.8	1.2	360	0.07
Total	–	531	2138	100	4.0	398	0.19

Consolidated surfaces are omitted, as they are sub-grid-cell features having a total estimated areal extent of <1%.

Table 2
Selected measured physical soil properties on hillslope surfaces in Tanh Minh (medians ± the median absolute deviation)

Landcover	N	K_s (mm h^{-1})	ρ_b (Mg m^{-3})	ϕ
Abandoned field	11	28 ± 10	1.09 ± 0.05	0.56 ± 0.03
Young secondary vegetation	13	32 ± 15	0.96 ± 0.05	0.63 ± 0.02
Forest	15	63 ± 31	0.97 ± 0.05	0.61 ± 0.03
Intermediate secondary vegetation	8	67 ± 39	1.02 ± 0.04	0.55 ± 0.03
Grasslands	11	93 ± 29	1.09 ± 0.05	0.57 ± 0.02
Upland field	17	103 ± 44	1.09 ± 0.05	0.57 ± 0.02

N: number of measurements; K_s: saturated hydraulic conductivity; ρ_b: bulk density; ϕ: porosity.

production and need – two to three times before a site is abandoned for an unspecified period. In some locations, fields extend down to the riparian zone, especially in zero-order catchments. In other locations, fields are bordered on the downslope side by vegetated patches (ranging in slope length from approximately 1–100 m), which potentially function as buffers. Hortonian overland flow is currently a somewhat common surface runoff generation mechanism on disturbed land covers (Ziegler et al., 2004); the HOF contribution to stream flow, however, is probably still small, compared with subsurface pathways. Buffering of overland flow on the hillslope, however, does not appear to be an intentional practice in Tanh Minh. In fact, the key determinants for villagers intentionally manipulating land-cover distribution seem to be need (e.g., planting on lands that are fertile enough to support two to three cycles) and deception—e.g., leaving enough trees in conspicuous locations (i.e., visible from the road) to satisfy government officials that no-forest-cutting policies are being obeyed. Detailed description of the agriculture system in Tanh Minh appears in other works (Rambo, 1996; Le Trong Cuc and Rambo, 1999; Fox et al., 2000, 2001).

3. Hortonian overland flow simulations

3.1. KINEROS2

We used the event-based, physics-based KINEROS2 runoff model (Smith et al., 1995, 1999) to simulate the generation and buffering of HOF during observed storms. KINEROS2 simulates water flow over a cascading system of watershed and hillslope elements (e.g., flow planes, channels, ponds). Overland flow is treated as a one-dimensional flow process, for which discharge per unit width (Q) is expressed in terms of water storage per unit area through the kinematic approximation:

$$Q = \alpha h^m \tag{1}$$

where α and m are parameters related to slope, surface roughness, and flow condition (laminar or turbulent) and h is the water storage per unit area. Eq. (1) is used in conjunction with the continuity equation:

$$\frac{\partial h}{\partial t} + \frac{\partial Q}{\partial x} = q(x,t) \tag{2}$$

where x is the distance downslope, t the time, and $q(x,t)$ is the net lateral inflow rate per unit length of channel. Solution of Eq. (2) requires estimates of time- and space-dependent rainfall $r(x,t)$ and infiltration $f(x,t)$ rates:

$$q(x,t) = r(x,t) - f(x,t) \tag{3}$$

Infiltrability is defined as the limiting rate at which water can enter the soil surface (Hillel, 1971). Modeling of this process utilizes several input parameters that describe the soil profile: e.g., K_s, integral capillary drive or matric potential (G), porosity, and pore size distribution index (Brooks and Corey, 1964). The general infiltrability (f_c) equation is a function of cumulative infiltrated depth (I) (following Parlange et al., 1982):

$$f_c = K_s\left[1 + \frac{a}{e^{(aI/B)} - 1}\right] \tag{4}$$

where a is a constant related to soil type (assumed to be 0.85 unless otherwise specified) and $B = (G + h_w)(\theta_s - \theta_i)$, for which h_w is surface water depth (computed internally) and the second term, unit storage capacity, is the difference of saturated (θ_s) and initial (θ_i) volumetric moisture contents (i.e., $\Delta\theta_i = \theta_s - \theta_i$). The expression $(\theta_s - \theta_i)$ is calculated as $\phi(S_{max} - S_i)$, where ϕ is porosity, and S_{max} and S_i are respectively the maximum and initial values of 'relative saturation', defined as $S = \theta/\phi$, or the fraction of the pore space filled with water. Antecedent soil moisture conditions in KINEROS2 are parameterized by assigning event-dependent values of relative saturation.

3.2. ESL simulations

The ESL simulations are designed to quantify the reduction in HOF generated on an upslope source area by downslope buffers occupying slope lengths ranging from 2 to 160 m. The upslope source area is a 30 m × 30 m abandoned field (AF). Similarly, the across-slope dimension of each buffer is 30 m. Fig. 4a shows the buffer arrangements considered. The longitudinal extent of the simulated hillslope varies from 32 to 190 m, depending on size of the downslope buffer. We used the 30 m × 30 m dimension for AF because it is a reasonable estimation of the size of individual fields on steep hillslopes in Tahn Mihn (personal observation). AF is used for the upslope surface because it has the lowest measured K_s of the major land covers (Table 2), and thus has the greatest propensity to generate HOF (Ziegler et al., 2004). This represents a worst-case scenario of HOF generation on typical, non-consolidated hillslope surfaces in the study area. The downslope land covers are the four vegetation types that commonly replace hillslope fields: young secondary vegetation, grassland, intermediate secondary vegetation, and forest (Appendix A). The output of each simulation is the overland flow that exits the downslope buffer (Fig. 4b). This value represents the HOF generated on the upslope field and not infiltrated in the downslope buffer; it also

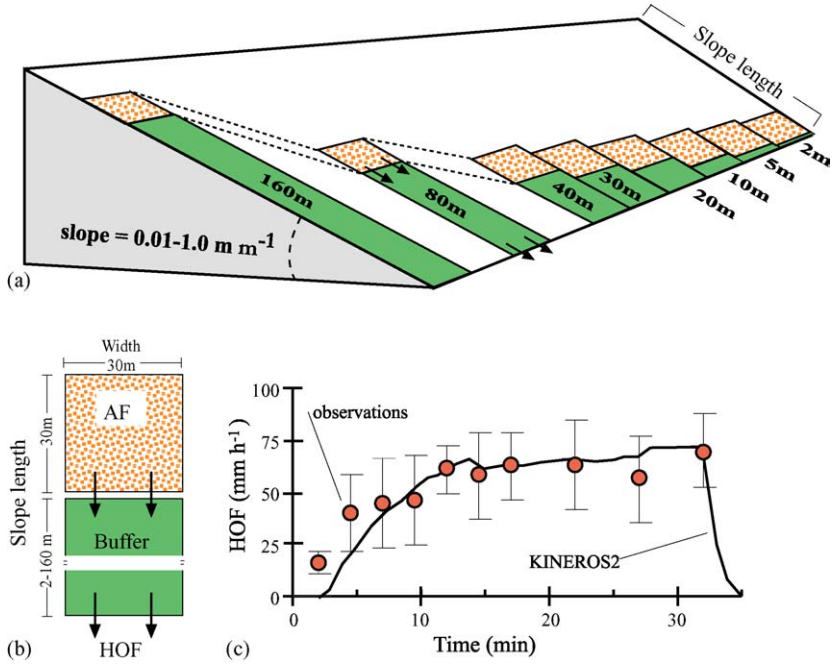

Fig. 4. (a) Conceptualization of the scenarios simulated. Slope lengths of the 18 buffers below the 30 m × 30 m abandoned field (AF) are 2, 5, 10, 20, . . ., 150, and 160 m; simulated slope angles are 0.01, 0.05, 0.10, 0.20, . . ., 0.90, and 1.0 m m^{-1}. (b) Arrangement of abandoned field and downslope land cover as represented in the KINEROS2 modeling framework; (c) comparison of KINEROS2-predicted HOF on the upslope agricultural field with results from field rainfall simulations in Thailand.

includes any HOF generated on the buffer. The time step for all simulations is 1 min, matching the measurement resolution of the rainfall record. We use a simulation time that is one hour longer than the storm duration to ensure that simulated HOF fully infiltrates into or drains from the downslope buffer.

We recorded 1-min rainfall intensities (I_1) using a MET-ONE (Grants Pass, OR) tipping bucket rain gauge (1 tip = 0.254 mm) and Campbell (Logan, UT) data logger from 26 March to 29 June 1998. Although short, this period encompasses the transition from the dry to the rainy season in Tanh Minh. Of 49 individual rainfall events recorded during this period, we classify 11 as 'storms' using a modification of the Wischmeier and Smith (1978) criteria (Ziegler et al., 2004). The storms are ranked according to maximum 30-min rainfall intensities (I_{30_MAX}) in Table 3. Based on similarity in 30-min maximum intensity values (I_{30_MAX}), we assigned the 11 storms to the following groups: large (number 1), medium (numbers 2, 3, 4, 5, 6, 7), small (numbers 8, 9), and very small (numbers 10, 11).

Before simulation, we calibrated KINEROS2 to predict runoff observed from small-scale plot experiments on an abandoned upland field in northern Thailand (Ziegler et al., 2000, 2001). Because we did not have such test data for the Vietnam field site, we used the Thailand runoff-plot data to ensure that KINEROS2 adequately simulated HOF generation response on an agriculture surface that is similar to the Tanh

Table 3
Eleven storm events recorded during the study period (26 March 1998–29 June 1998)

Storm	Class[a]	Start[b] (date/time)	End (date/time)	Duration (min)	Total (mm)	Average (mm h^{-1})	I_{1_MAX}[c] (mm h^{-1})	I_{10_MAX} (mm h^{-1})	I_{20_MAX} (mm h^{-1})	I_{30_MAX} (mm h^{-1})	I_{60_MAX} (mm h^{-1})
1	L	6/4 17:21	6/5 4:46	686	66.8	5.8	106.7	85.3	70.9	56.9	38.9
2	M	5/19 9:48	5/20 8:16	455	28.7	3.8	76.2	45.7	37.3	32.0	22.2
3	M	5/28 5:03	5/28 7:18	136	30.7	13.6	73.0	42.7	37.3	31.5	19.9
4	M	6/9 16:03	6/10 1:04	542	38.6	4.3	76.2	45.7	38.9	30.7	22.9
5	M	6/7 16:06	6/7 17:31	86	18.3	12.8	61.0	44.2	37.3	30.5	18.1
6	M	5/31 6:16	5/31 2:44	389	21.8	3.4	121.9	44.2	30.5	26.2	13.8
7	M	5/18 7:15	5/18 8:02	48	14.2	17.8	121.9	57.9	35.4	25.4	–
8	S	5/5 15:22	5/5 17:20	119	16.5	8.3	106.7	33.0	22.1	21.3	14.8
9	S	5/23 23:31	5/24 5:24	954	42.4	2.7	45.7	27.4	19.8	19.8	16.5
10	VS	5/30 23:24	5/31 7:11	468	16.8	2.1	61.0	16.0	12.6	11.9	10.5
11	VS	6/10 20:45	6/11 4:44	480	14.5	1.8	61.0	15.2	13.0	9.2	4.9

[a] Storms are ranked according to I_{30_MAX} values; class refers to an arbitrary classification of large (L), medium (M), small (S), and very small (VS) storms.
[b] Date/time format is month, day, hour, and minute.
[c] I_{1_MAX}, I_{10_MAX}, I_{20_MAX}, I_{30_MAX}, and I_{60_MAX} refer to maximum 1-, 10-, 20-, and 30- and 60-min rainfall intensities.

Table 4
Parameters used for the buffer simulations with KINEROS2

Landcover	Code	K_s[a] (mm h^{-1})	C_v	ϕ	n	C_a	Int (mm)
Abandoned field	AF	28	0.36	0.57	0.13	0.50	0.25
Young secondary vegetation	YSV	32	0.47	0.63	0.20	0.75	1.65
Forest	F	63	0.49	0.61	0.15	0.85	1.80
Intermediate secondary veg.	ISV	67	0.58	0.55	0.20	0.80	1.75
Grasslands	GL	93	0.31	0.57	0.24	0.90	2.00
Upland field	UF	103	0.39	0.57	0.05	0.10	0.50

[a] Variables are saturated hydraulic conductivity (K_s); the coefficient of variation for K_s (C_v); porosity (ϕ); Manning's n, vegetation coverage (C_a), total interception depth by the vegetation (Int). Values of K_s, C_v, and ϕ are those from Table 2. Manning's n is determined from field observations compared with values in Morgan, (1995); C_a values are based on field surveys; Int is inferred by comparing field observations with values from Horton (1919). The following are the same for all land covers (based on field observations): volumetric rock fraction (1%), average microtopography relief (2 mm), average microtopography spacing (0.3 m).

Minh site. We recognize this is an important limitation, but we believe that this type of ''testing'' is better than none. The thick line in Fig. 4c shows the KINEROS2 simulation of runoff. Observed runoff values, represented by circles, are the means of four replications. Total error, error in the peak estimate, and root mean squared error for the KINEROS2 predictions were acceptable: <1%, 4.5%, and 16.7%, respectively.

The ESL simulations are performed by replacing parameter values from the Thailand calibration runs with those obtained from field measurements on the six hillslope landcover types in Tanh Minh (Table 4). Some of these values are the field-measured values—i.e., those in Table 2. All simulations assume a particle density of 2.49 g cm^{-3}, which is the median of 13 measurements taken on several hillslopes. Other parameters are determined by comparing field observations of surface/vegetation characteristics to published values. Values for pore size distribution index (0.25) and capillary drive, for example, are based on those reported by Rawls et al. (1982) for sandy clay loam, the most commonly found soil texture on Tanh Minh hillslopes. The final capillary drive value (82.58 cm) was modified from the originally assigned value during model calibration. Therefore, it is the only parameter in the final simulations that is determined by calibration using the Thailand data. Additional parameter determination methods are provided in the footnote of Table 4. For all events we use a relative saturation value equal to the field capacity value (0.67 for sandy clay loam soil, Woolhiser et al., 1990).

4. Results

4.1. Buffer effectiveness

Two examples of simulation results are shown in Table 5. Simulated HOF depths for four types of hillslope buffers of variable length are shown for the largest storm (no. 1) and one medium storm (no. 4). Total rainfall (mm) and predicted HOF on the upslope 30 m × 30 m abandoned field (mm) are shown below the storm identifier. Simulated slope angle is 0.5 m m^{-1}; simulation time step is 1 min. Overland flow passing through each downslope land cover is listed as a depth for the 18 buffer lengths considered. Buffer effectiveness (BE) of each downslope land cover of variable length is calculated as

$$\mathrm{BE} = \frac{\mathrm{HOF_{AF}} - \mathrm{HOF_{AF\rightarrow buffer}}}{\mathrm{HOF_{AF}}} \times 100\% \quad (5)$$

where $\mathrm{HOF_{AF}}$ is the KINEROS2-simulated HOF (mm) on the upslope abandoned field only; $\mathrm{HOF_{AF\rightarrow buffer}}$ is the simulated HOF (mm) passing through the downslope slope buffer (i.e., that shown in Fig. 4b).

The simulations of HOF and BE are presented for storm numbers 1 and 4 in Fig. 5. Simulated HOF depth for all buffer scenarios increases monotonically with increasing slope angle (not shown). Apparent in the results are the following: (1) a comparatively high depth of simulated HOF is generated during the large storm 1, compared with the medium-sized storm 4; (2) BE increases as buffer slope length increases; (3) intermediate secondary vegetation, natural forests, or grassland are more effective buffers than young secondary vegetation. This latter point is shown clearly in Fig. 5d, as BE for YSV only reaches 85% for buffers >150 m. In comparison, BE > 85% for relatively short slope lengths for the other three types of buffers. The BE patterns for GL, ISV, and F are practically indistinguishable for buffer lengths >20 m. These trends are generally true for all other simulated storms (not shown).

4.2. ESL determination

In our ESL determination, we focus on the BE values determined during the simulation of the six medium-sized storms. Collectively, this group of storms covers a wide range of rainfall phenomena in Tanh Minh (e.g., long-duration events, short high-intensity bursts exceeding 120 mm h^{-1}; relatively high hourly maximums). Large storm 1 is used to verify the ESL selections. In Fig. 6, effectiveness values (circles) for all GL buffers and slope angles considered are shown for simulated storm 4. The thick line is simply fit through the BE values for the 0.5 m m^{-1} slope gradient. We identify the ESL to be the length where BE ≥ 85%. For this example, the threshold effectiveness occurs at approximately 47 m. In the comprehensive ESL determination, we calculate BE values for all six medium-sized storms, 11 slope angles, and 18 buffer lengths. Again, the value identified in Fig. 6 represents only one of these cases.

Table 5
KINEROS2-predicted HOF during the largest and one medium storm

Events[a]	Buffer slope length	Downslope land cover[b]			
		YSV (mm)	ISV (mm)	F (mm)	GL (mm)
Storm 1; RF: 66.8 mm; AF HOF: 7.9 mm	2	7.13	5.72	5.90	5.38
	5	6.77	4.37	4.60	3.08
	10	6.15	2.38	2.68	1.16
	20	5.30	0.67	0.90	0.51
	30	4.66	0.41	0.53	0.40
	40	4.14	0.35	0.39	0.36
	50	3.79	0.32	0.35	0.32
	60	3.45	0.28	0.31	0.27
	70	3.10	0.25	0.27	0.23
	80	2.75	0.22	0.23	0.18
	90	2.60	0.21	0.22	0.17
	100	2.46	0.21	0.21	0.17
	110	2.31	0.20	0.20	0.16
	120	2.16	0.20	0.19	0.16
	130	2.01	0.19	0.18	0.15
	140	1.86	0.18	0.18	0.14
	150	1.71	0.18	0.17	0.14
	160	1.56	0.17	0.16	0.13
Storm 4; RF: 38.6 mm; AF HOF: 1.4 mm	2	1.03	0.65	0.73	0.66
	5	0.89	0.40	0.48	0.36
	10	0.69	0.24	0.28	0.23
	20	0.51	0.14	0.16	0.13
	30	0.43	0.10	0.10	0.09
	40	0.38	0.08	0.08	0.07
	50	0.35	0.07	0.08	0.06
	60	0.32	0.06	0.07	0.06
	70	0.29	0.06	0.06	0.05
	80	0.26	0.05	0.05	0.04
	90	0.25	0.05	0.05	0.04
	100	0.23	0.05	0.04	0.04
	110	0.22	0.04	0.04	0.04
	120	0.21	0.04	0.04	0.03
	130	0.20	0.04	0.04	0.03
	140	0.19	0.04	0.03	0.03
	150	0.18	0.04	0.03	0.03
	160	0.16	0.04	0.03	0.03

[a] Event information includes storm number (see storm data in Table 3), total rainfall, KINEROS2-predicted HOF from the 30 m × 30 m abandoned field (AF) situated above each of the downslope land covers. Simulated slope angle is 0.5 m m^{-1} for this example.
[b] Abreviations are for the following land covers: young secondary vegetation (YSV), intermediate secondary vegetation (ISV), grassland (GL), and forest (F).

The results of this comprehensive analysis of ESL are summarized in Fig. 7. The thick line defines the predicted ESL for slope angles up to 1 m m^{-1}. The thin solid line is simply 30 m longer than the ESL length, reflecting the length of the simulated abandoned field upslope. The ESL (m) is approximated with the following logarithmic regression equation:

$$\mathrm{ESL} = 98 + 15\ln(\mathrm{slope}) \quad (6)$$

where slope angle is m m^{-1}, $R^2_{adj} = 0.95$. Eq. (6) predicts ESL values ranging from 29 to 98 m over the slope-angle range 0.01–1.0 m m^{-1} (note: for flatter slopes one should use slope = 0.01 m m^{-1}).

4.3. Comparison with other ESL indices

A comparison of our simulation-based ESL (thick, solid line) with data from other regions is shown in Fig. 8. The closed circles are case-study values reported by Haupt (1959), van Groenewoud (1977), Chalmers (1979), Balmer et al. (1982), and Plamondon (1982). The thin, solid lines are derived from summary data reported by Lee et al. (2004) for mostly non-tropical forests in the USA and Canada: Boreal, Pacific (PAC), Northeast (NE), Midwest (MW), Rocky/Intermountain (Rocky), and Southeast (SE). For clarity, the similar PAC, NE, and MW data are presented as one line; the SE data, which plot closely along the T–S line, are not shown. Collectively, the USA/Canada data are derived from the guidelines of 60 management jurisdictions in those two countries (Lee et al., 2004), and therefore, reflect contemporary buffer practices. The broken T–S line is the relationship presented by Trimble and Sartz (1957) for estimating buffer 'width' (m) from slope gradient (m m^{-1}); it can be represented as

$$\mathrm{width} = 60\,\mathrm{slope} + 8.0 \quad (7)$$

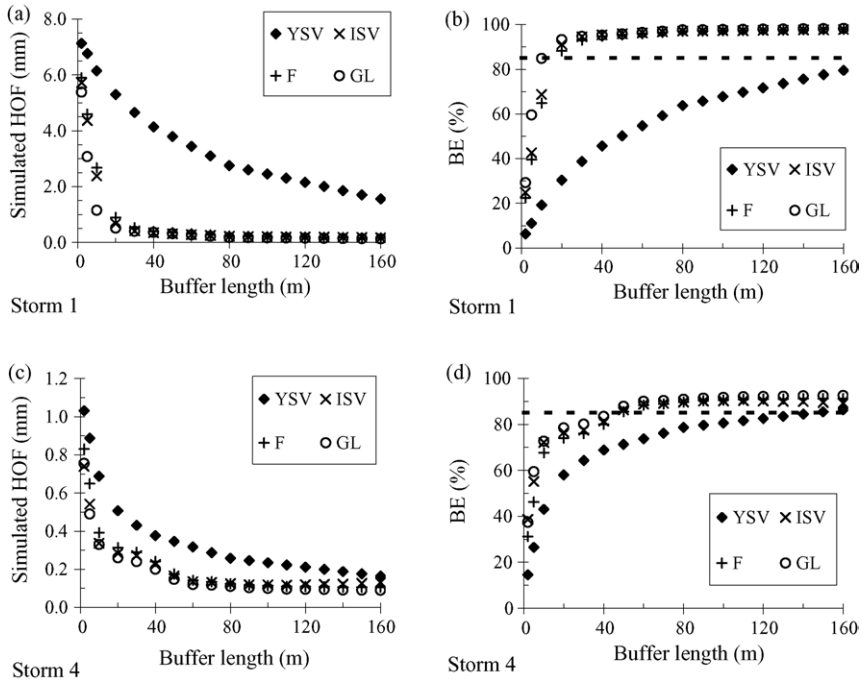

Fig. 5. Panels (a) and (c) show simulated HOF during storms 1 and 4 for various lengths of downslope buffers (Table 5). Simulated slope angle is 0.5 m m^{-1}. Panels (b) and (d) show buffering effectiveness values computed via Eq. (5) for the simulations shown in Panels (a) and (c). The dotted line indicates a threshold effectiveness of 85%. The downslope land covers are young secondary vegetation (YSV), intermediate secondary vegetation (ISV), forest (F), and grassland (GL).

Eq. (7) has been used as a general guideline in Australia for assigning buffer width (Clinnick, 1985; Barling and Moore, 1994). In general, the T–S line plots below our ESL and most of the summarized values from the other indices (lines) and experimental data (closed circles).

Different from all the other slope-specific relationships is our use of the natural log function to specify ESL. Again, this is based on HOF simulations, not in situ observations. This curve specifies comparatively longer buffers for smaller slope angles than the other methods. We feel this is appropriate because hillslope erosion in the tropics initially increases rapidly as slope increases from gentle to moderate slopes (p. 35, Morgan, 1995); observations supported that this was also generally the case at Tanh Minh.

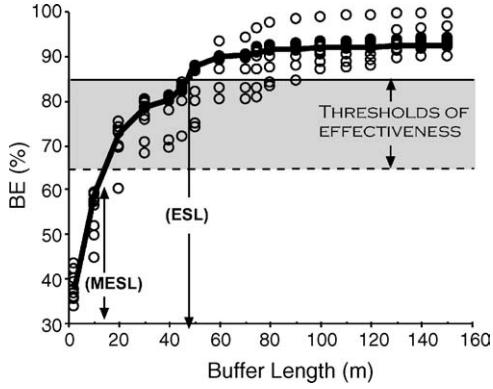

Fig. 6. Buffer efficiency calculated (Eq. (5)) for storm 4 for the scenario of a down-slope grassland buffer of various lengths. Data for 11 simulated slope angles are shown; the thick line highlights the values for the simulation of a 0.5 m m^{-1} slope. Two levels of buffer effectiveness are indicated at 85 and 65%. The former is used herein to identify the ESL (i.e., Eq. (6)); the latter, the MESL (Eq. (8)).

5. Factors affecting ESL determination

Herein we focus on infiltration of simulated HOF generated during observed storms to establish an effective slope length for hillslope buffers in the Tanh Minh study area. In doing so, we

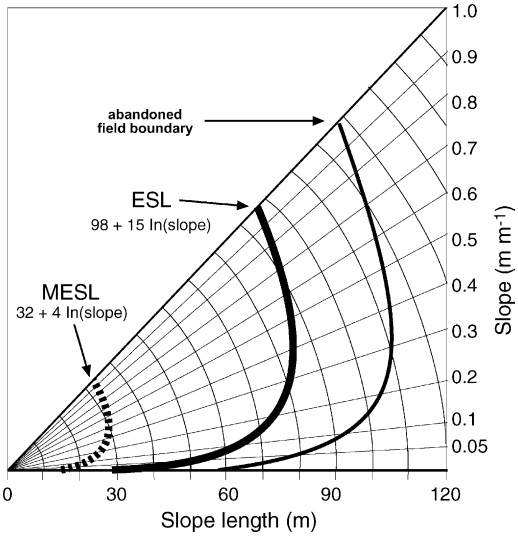

Fig. 7. The effective slope length (ESL) is determined via Eq. (6) for slope angles up to 1 m m^{-1} (thick line) The thin solid line reflects extent of the abandoned field, which is the upslope HOF source area in the ESL simulations. The minimum effect slope length (MESL; dotted line; via Eq. (8)) is a less conservative estimate of the buffer length required to infiltrate overland flow on hillslopes in the study area.

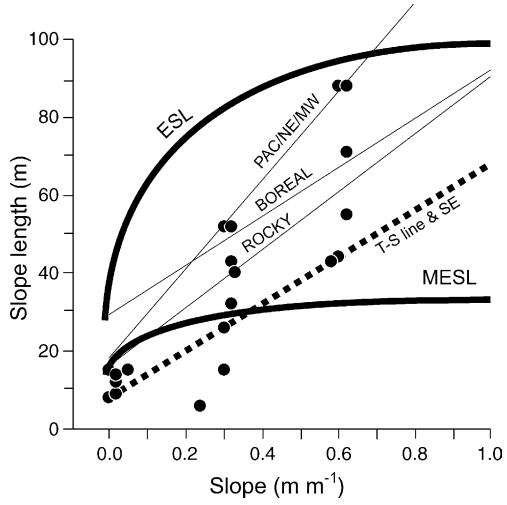

Fig. 8. Effective slope length (ESL) and minimum effective slope length (MESL) are compared with data/guidelines from other studies or reviews. The dashed line is the relationship of Trimble and Sartz (1957). The thin lines represent the compiled data for contemporary practices in several regions with the USA and Canada (Lee et al., 2004): Boreal, MW (Midwest), NE (Northeast), PAC (Pacific), ROCKY (Rocky and intermountain), and SE (Southeast; plotted along the T–S line for clarity). The closed circles are specific buffer lengths that were identified in field-based studies (Haupt, 1959; van Groenewoud, 1977; Chalmers, 1979; Balmer et al., 1982; Plamondon, 1982).

make assumptions regarding the following inter-related phenomena that affect buffering: (1) physical properties of buffers; (2) antecedent soil moisture and hydrologic conditions within the buffer; (3) topography and soil depth; (4) type of overland flow. These factors and their influence on our determination of an ESL via diagnostic modeling are discussed in the following sub-sections.

5.1. Physical characteristics

The collective processes affecting the filtering of sediments by a vegetated buffer are not entirely the same processes that reduce overland flow transport in our KINEROS2 simulations. Filtering in general is achieved both through the infiltration of water entering the buffer from upslope and via the physical blocking of flowing water by the vegetation comprising the buffer (Phillips, 1989; Meyer et al., 1995). The former process may also be facilitated by the latter. Entrained sediment is deposited in the buffer, for example, because infiltration-induced reduction in flow decreases sediment transport capacity. Similarly, the vegetation itself forms a physical barrier to flowing water, such that particle settling occurs once settling velocity exceeds flow velocity. The influence of blocking is related to vegetation height, stiffness, percentage cover, above/below ground biomass, and vegetation density.

Our KINEROS2 simulations address infiltration, which, via Eq. (4), is primarily a function of saturated hydraulic conductivity. Parameterized physical characteristics of the buffer vegetation affect overland flow in the KINEROS2 model indirectly by influencing canopy interception loss and ponding depth. The assignment of Manning's n and average micro-topographic relief/spacing surface parameters do however directly influence flow characteristics. Had our analyses focused on the filtering of some specific material rather than reducing HOF, a different value for ESL may have emerged (e.g., a buffer for filtering coarse-sediment would likely have been shorter). A model like KINEROS2, however, lacks the complexity to simulate specific filtering processes, unless they are functions of the transport capacity of flowing water (cf. Dillaha and Hayes, 1991; Srivastava et al., 1998). Other models may be more appropriate in this respect (e.g., Munoz-Carpena et al., 1999; also see Flanagan et al., 1986, 1989; Hayes and Dillaha, 1992; Lin et al., 2002).

5.2. Antecedent conditions

Prevailing hydrologic conditions influence buffer effectiveness (Munoz-Carpena et al., 1999). For example, if a riparian buffer is saturated by an elevated water table or by the capillary fringe (O'Loughlin, 1981), both rainfall and run-on water will not infiltrate in this zone. In our buffer simulations, we assume no influence of the water table on the downslope buffers, as KINEROS2 does not model this process explicitly.

Important, however, is our handling of antecedent moisture. For wet-versus-dry conditions, less water is infiltrated before the occurrence of ponding, after which infiltration rate is governed by the saturated hydraulic conductivity of the soil. During wetter conditions, therefore, buffer effectiveness should be reduced because: (1) the total volume of HOF that can be infiltrated by the buffer is reduced and (2) more HOF will likely be transported into the buffer from the upslope source. This effect can be seen clearly in Fig. 9, where simulated HOF from storm 1 for various antecedent moisture conditions is shown.

To ensure ample HOF generation in our ESL simulations, we use an initial soil moisture value equivalent to field capacity.

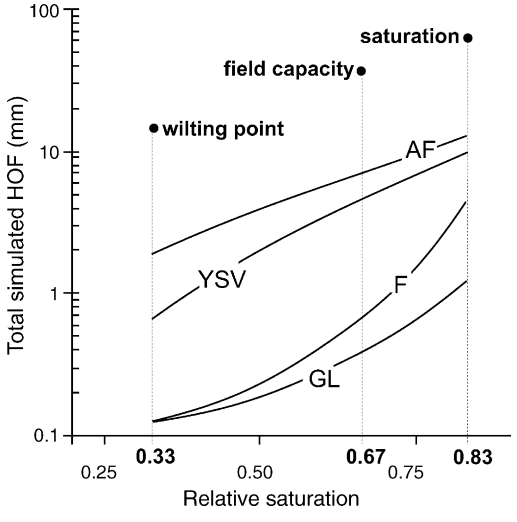

Fig. 9. KINEROS2-predicted HOF for four 30-m buffer covers for varying degrees of antecedent soil moisture during storm 1. Soil moisture is represented as the KINEROS2 relative saturation value for a sandy clay loam soil. Values for wilting point, field capacity, and saturation conditions are from Woolhiser et al. (1990). Dimensions of the abandoned field are 30 m × 30 m; the downslope buffers are of equal dimension. The four scenarios represent the range of K_s values found on downslope land covers in Tanh Minh (≈30–90 mm h^{-1}).

Vertessy et al. (2000) caution that initial soil moisture is one of the most important parameters affecting the outcome of simulated runoff (Stephenson and Freeze, 1974), for which the influence may also be dependent on storm size (Merz and Bardossy, 1998). Our interpretations of buffer effectiveness account for this influence. If a different value of initial soil moisture were used, the magnitude of the simulated HOF values would change—e.g., decrease in the case of using the wilting point value. We assume, however, that the response patterns of BE that we use to determine the ESL, would be similar.

5.3. Topography and soil depth

Our analyses are based on simulations of planar hillslopes with fixed soil depths. As a result, we ignore additional inputs from return flow emerging at breaks in topography or saturation overland flow (SOF) occurring at hillslope convergence points and/or shallow soil locations. In part, we ignore these overland flow generation processes to focus on Hortonian overland flow, which from prior work we know occurs during some storms (Ziegler et al., 2004). In our parameterization of the soil profile for the KINEROS2 simulations, we use a soil depth of 2 m (based on observations); this depth prevents any modeled source or buffer element from becoming saturated during the storms considered. In addition, the few locations in Tahn Minh where we observed either return flow or SOF were at hillslope positions that were connected directly to the stream system (e.g., concave hollows of zero-order basins). At these locations, the types of buffers we are simulating herein would have limited opportunity to infiltrate overland flow. Riparian-type buffers, which do not fall within the scope of this paper, may however be effective in filtering sediments (cf. Castelle et al., 1994; Gilliam, 1994).

5.4. Shallow unconcentrated versus concentrated overland flow

One of the most important factors controlling buffer effectiveness is the nature of overland flow entering the buffer: i.e., shallow unconcentrated overland flow (SUOF) versus concentrated overland flow (COF). Concentrated flow can pass through downslope buffers because the total depth of run-on water passes over a smaller spatial area (cf. Dillaha et al., 1989; Dosskey et al., 2002). COF typically moves within rills that channel water around potentially restricting features. Flow velocity can be considerably higher than for SUOF. In some instances, the concentration of overland flow by the plant cover may accelerate erosion within the buffer (De Ploey et al., 1976). Welsch (1991) noted that COF should be converted to SUOF before entering a riparian buffer to provide a more effective system.

In our simulations, we assume all overland flow is SUOF, the type simulated on solitary planes by KINEROS2. Field observations demonstrate that our treatment of overland flow in the K_s-based simulations is not a perfect representation of actual conditions. For example, one questions whether SUOF is prevalent on irregular-shaped, vegetated hillslopes – and in particular, for distances up to 30 m, the length of the simulated upslope field. Additionally, our simulations for idealized hillslopes might over-estimate HOF because of the artificial 'smoothness' imposed; natural slopes with even small irregularities would tend to cause more runoff to re-infiltrate on hillslopes. We observed COF generation in Tanh Minh during sustained periods of high rainfall intensity on some abandoned fields; however, it was most prevalent at hillslope concentration points (e.g., discharge locations from paths and rock outcrops).

For the ESL determination, our consideration of a very short rainfall record may lead us to underestimate the buffer length required to infiltrate surface runoff from large annual events. These large events tend to facilitate generation of COF. It was simply not tractable to simulate all conditions. In some respect, our use of a low-K_s upslope surface and a relatively high initial soil moisture value (field capacity), represent a worst-case scenario for overland flow generation. Nevertheless, in the case of concentrated overland flow, buffer effectiveness would be less than our simulations indicate—even the filtering ability of exceptionally long buffers can be compromised by COF (cf. Dillaha et al., 1989; Magette et al., 1989). The reported ESL values should facilitate reduction of overland flow augmented by other sources (e.g., return flow), so long as the flow does not concentrate.

One notable example of overland flow passing through downslope buffers in Tanh Minh involves the occurrence of two grass species, *Miscanthus japonicus* (Thunb.) And. (Gramineae) and *Saccharum spontaneum* L. (Gramineae). These grasses (≈1.0–2.5 m tall) are often found on former hillslope fields in isolated clumps with minimal vegetation growing in the shaded areas between. Overland flow circumvents the grass clumps (area $\leq \approx 1$ m^2) by flowing within well-formed rills as COF. Even for the case of SUOF entering from above, the existing rill system may concentrate flow, pre-empting any opportunity for infiltration to occur. In contrast, the grass species *Microstegium vagans* (Nees ex Steud.) A. Camus (Gramineae) forms a thick, uniform cover that blocks runon water and limits rill formation, thereby limiting the concentration of overland flow within the buffer.

6. Minimum effective slope length (MESL) for a buffer

From a practical standpoint, the comparatively long ESL values determined by Eq. (6) may not be accepted by farmers who already have limited lands for cultivation. Non-adoption of seemingly beneficial conservation practices for reasons related to cost, practicality, convenience, and understanding is common in upland areas of Southeast Asia (Garrity et al., 1998; Fahlen, 2002). Thus, there is utility in exploring the effectiveness of shorter buffers. In the example shown in Fig. 6, we identify a lower threshold of buffer effectiveness at 65%—i.e., 17 m. In a second set of analyses we determine the minimum effective slope length (MESL) in the same manner as the ESL determination, but using the criteria of BE $\geq$ 65%. MESL values (m) are approximated by the following logarithmic regression equation:

$$\mathrm{MESL} = 32 + 4\ln(\mathrm{slope}) \quad (8)$$

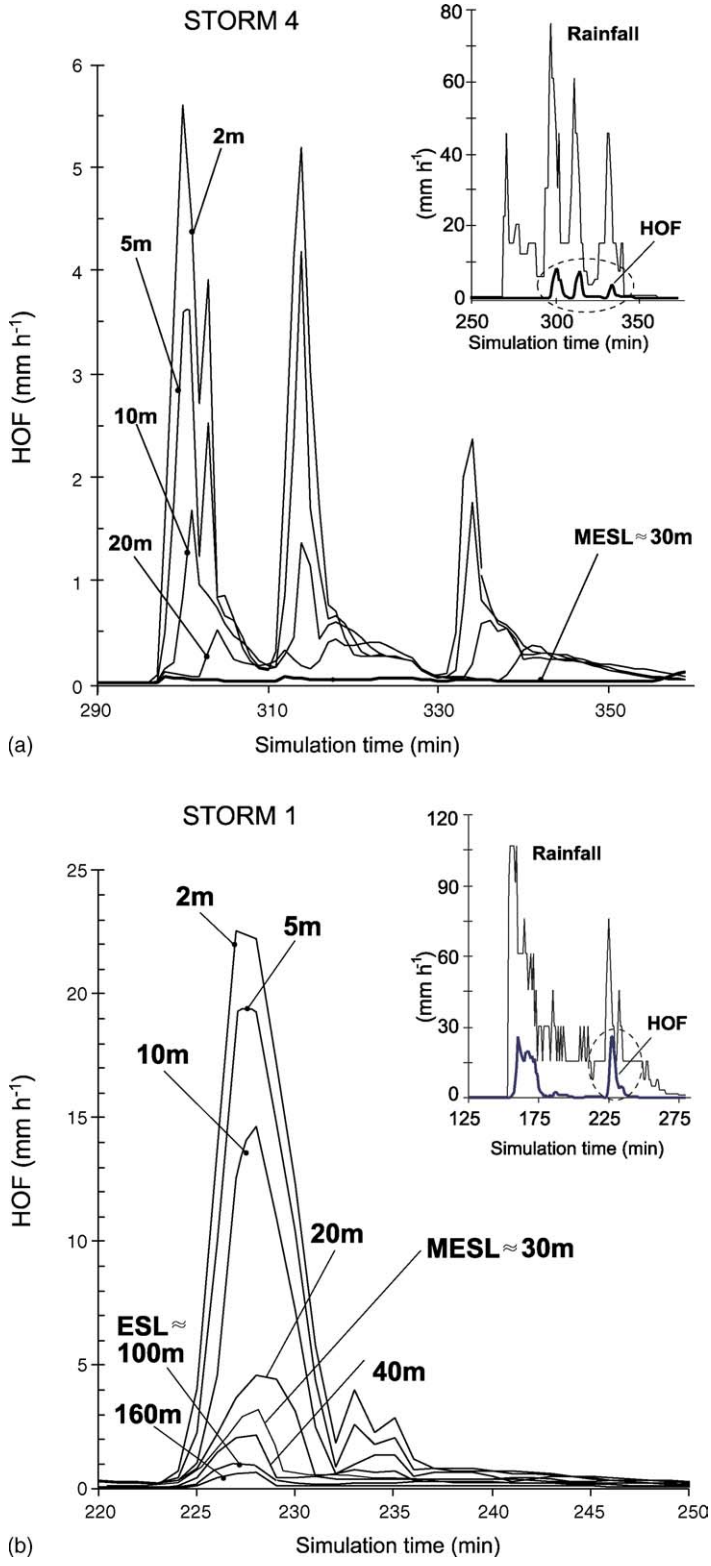

Fig. 10. Effectiveness of various buffer widths of the Forest land-cover during the KINEROS2 ESL simulations for (a) storm 4, one of the largest medium-sized observed storm and (b) storm 1, the largest observed storms. Storms are described in Table 3. The ESL and MESL refer to the effective slope length (ESL) and minimum effective slope length (MESL) for the simulated hillslope (slope angle = 0.8 m m^{-1}); they are 95 and 31 m, respectively. The insets in each panel show the relationship of HOF response to rainfall patterns; the dotted circle indicates the simulation time period shown in the main figure.

As before, slope angle is m m^{-1}, R^2_{adj} is 0.69. Eq. (8) predicts a buffer length of 14 m for a slope gradient of 0.01 m m^{-1}, and 23–32 m, for slope angles ranging from 0.10 to 1.0 m m^{-1} (Fig. 7).

Several field studies report the effectiveness of buffer lengths on the order of 20–30 m (Wylie, 1975; Erman et al., 1977; Graynoth, 1979; Davies and Neilson, 1994). In their respective reviews, Clinnick (1985) and Barling and Moore

(1994) concluded that the most commonly recommended slope length for stream buffers is 30 m. Lee et al. (2004) report that mean buffer widths in the USA and Canada vary from about 15 to 30 m, depending on the water body protected and the associated forest type. Castelle et al. (1994) note that a minimum effective buffer slope length of 15 m is needed to protect wetlands and streams under most conditions (cf. Herron and Hairsine, 1998).

The simulated effectiveness of 20 and 30 m buffers in Tahn Minh during the medium storm no. 4 is shown in Fig. 10a, where the filtering achieved by various lengths of a forest buffer is compared. Slope angle in this example is 0.8 m m^{-1}. Only negligible amounts of HOF generated during three rainfall bursts of storm no. 4 pass through the 30-m buffer, demonstrating that this length is near the threshold at which simulated HOF from all but the largest observed storms in Tanh Minh can be infiltrated. Thus, for medium-sized or smaller storms, the MESLs provide reasonable protection, even for this relatively steep gradient. However, it is during the rare, larger storms that filtering of overland flow is most crucial. For the largest storm (storm no. 1, Fig. 10b), which generated 7.9 mm of simulated HOF on the 0.8 m m^{-1} slope, longer buffer lengths are required to achieve adequate reduction in simulated HOF generated on the 30-m upslope abandoned field.

Herron and Hairsine (1998) recognize that disproportionately large buffers may be needed for highly disturbed sites. In Tanh Minh, our simulations suggest that long buffers are needed for infiltrating HOF generated on relatively small, disturbed upslope source areas. Disturbances on tropical soils in general may produce more overland flow than disturbances in temperate locations with similar topography, largely due to the higher decomposition rates and thinner organic horizons (cf. Sidle et al., this issue). Smaller buffer strips may therefore be sufficient in other locations with comparatively deep organic horizons with high infiltration capacities.

7. Implementation

Our ESL/MESL values represent initial estimates of appropriate slope lengths for hillslope buffers at the Vietnam field site. The derivation of these values was greatly affected by our parameterization of the physical situation at Tahn Minh. Those using such an approach outside of this study area should first consider 'on-ground' assessments to account for differences in surface conditions (cf. Lin et al., 2002; Tomer et al., 2003). A thorough understanding of the hillslope hydrological and geomorphological processes is needed to design the buffers to handle the magnitude of expected flows. Site assessments should consider all relevant bio-geo-hydro-climatic factors, including the following:

- Precipitation and soil variables affecting runoff generation (intensity/duration relationships for rainfall; spatial variation in saturated hydraulic conductivity, soil depth, bulk density, aggregation, porosity, and extent of preferential flow for soil).
- Surface conditions on the hillslope that affect ponding, infiltration, or movement of surface water (e.g., woody debris, microtography, terracing, surface sealing, rock cover, litter depth/condition).
- Surface evidence that elucidates flow pathways—in some cases, mapping of surface erosion features (e.g., rill density/depth) and overland flow pathways may serve as a general guide for determining necessary hillslope buffer dimensions.
- Additional sources of overland flow, such as return flow occurring at topographic breaks, saturation overland flow forming at points of hillslope convergence and/or shallow soil locations, and runoff entering the hillslope from disturbed surfaces such as roads, paths, and rock outcrops.
- Concentrated sediment sources, such as gullies and potential landslides and debris flows all of which may preclude most natural buffers for stream protection.
- Spatial and temporal distributions of future land-use activities and/or disturbance that will alter the physical characteristics of the buffer (once established) or the upland source areas for HOF—e.g., swidden agriculture, timber extraction, and grazing are important in many tropical highland basins.
- Physical characteristics of the probable buffer type (hillslope versus wetland) and buffer vegetation (e.g., see discussion in Section 5.4 regarding *Miscanthus japonicus* versus *Microstegium vegans*).

Finally, buffers should be regarded as conservation practices that complement the land management activities on the hillslope and watershed as a whole (Barling and Moore, 1994; Herron and Hairsine, 1998). Sound conservation involves more than simply locating fixed-dimension buffers between streams and sources (Bren, 2000; Tomer et al., 2003). Additionally, the specific objectives of the buffer should be considered—i.e., is it designed solely to infiltrate overland flow or must other 'filtering functions' be considered (e.g., sediments, nutrients, chemicals, bacteria).

8. Summary

Through diagnostic computer simulations of overland flow generation with the KINEROS2 runoff model using field data, we determine the effective slope length (ESL) required by vegetated buffers to infiltrate overland flow on disturbed hillslopes in two fragmented basins of northern Vietnam. The ESL values are estimated from slope gradient (applicable range = 0.01–1.0 m m^{-1}) using the following equation: ESL = 98 + 15 ln(slope). Specification of buffer slope length using a logarithmic curve is more appropriate for our tropical site than using a linear-based function of slope angle because it assigns longer buffers at lower slope angles where overland flow and erosion processes begin to be significant on degraded hillslopes. For areas with less disturbance or locations where long buffers cannot be implemented, we estimate the minimum effective slope length (MESL = 32 + 4 ln(slope)) needed for hillslope buffers on the same range of slopes. Our diagnostic analyses, however, suggest that such shorter buffers would be considerably less effective during large storm events than those determined by the ESL criteria.

Although the ESL approximations are intended to be a guide for developing buffers on disturbed hillslopes at the Vietnam study site, they may be applicable to similar landscapes in other disturbed montane tropical areas. However, one should understand the assumptions and limitations of our approach. The ESL determinations originate from computer simulations focusing on the infiltration of shallow, unconcentrated Hortonian overland flow by three types of buffering vegetation common to disturbed hillslopes in the Vietnam study area (grassland, forest, and intermediate secondary vegetation). Furthermore, we considered only one fixed-sized overland flow source (a 900-m^2 abandoned field). We focus on Hortonian flow because it is currently an important mechanism for overland flow generation on disturbed hillslopes in the study area. Buffer effectiveness depends on slope angle, physical characteristics of the downslope buffer (e.g., length, vegetation coverage, surface roughness, K_s), storm characteristics (e.g., sustained intensity, antecedent soil moisture), and the type and volume of overland flow entering the buffer (unconcentrated versus concentrated flow). Because our simulations of shallow unconcentrated flow are not able to account for all of these factors explicitly, the identified ESL values may not even be appropriate for all sites within the study area. For example, our estimated ESL would not likely be appropriate for hillslopes with abrupt changes in topography, soil depth variations, or other phenomena that are conducive to return flow generation. In addition, greater volumes of overland flow generated on source areas larger than the one we considered herein would likely require longer buffers than indicated by our ESL approximations.

The final determination of buffer size (and hillslope placement) should consider site-specific observations of all phenomena that affect the generation, movement, and infiltration of overland flow. Additionally, buffers determined by ESL-criteria should be used in conjunction with other hillslope conservation techniques. Large overland flow source areas occurring on long slopes, for instance, may require multiple and staggered buffers. In the case of concentrated overland flow, such as that generated during exceptionally large events or that entering the hillslope from a road or another type of compacted surface, effectiveness of any practical length of buffer would likely be compromised.

Finally, in the context of understanding the hydrological consequences of landscape fragmentation, even relatively small buffers (e.g., on the order of our MESL estimates) have the ability to infiltrate some of the HOF generated on upslope source areas of limited size. This has important implications for how land-cover juxtaposition and degree of fragmentation affect overland flow generation and movement on fragmented hillslopes.

Acknowledgments

This paper results from joint work conducted by researchers from the University of Hawaii, East–West Center (Honolulu, HI), and Center for Natural Resources and Environmental Studies (CRES) of the Vietnam National University, Hanoi. Financial support for the Hawaii-based team was provided by a National Science Foundation Grant (no. DEB-9613613). Alan Ziegler was supported by an Environmental Protection Agency STAR fellowship. We thank the following for support during the project: Lan, Lian, Mai, and Tranh Bin Da (field work); Jefferson Fox, Don Plondke, and Stephen Leisz (GIS and remote sensing); Le Trong Cuc, Nghiem Phuong Tuyen, and the other CRES staff in Hanoi; Jitti Pinthong, Chiang Mai University, Thailand (soil taxonomic description); J.F. Maxwell (taxonomic nomenclature); Carl Unkrich, Southwest Watershed Research Center, USDA-ARS, Tuscon AZ (help with KINEROS2); finally, all the Tay villagers who welcomed us in their community. An early incarnation of this paper benefited from critical review by Sampurno Bruijnzeel (Free University, Amsterdam).

Appendix A. Vegetation descriptions for several land covers

Upland field (UF): Active fields, including banana (*Musa coccinea* Andr. (Musaceae), *Musa paradisiacal* L. (Musaceae)), and canna (*Canna edulis* Ker (Cannacea)), cassava (*Manihot esculenta* Grantz (Euphorbeaceae)), corn (*Zea mays* L. (Gramineae)), and rice (*Oryza sativa* L. (Gramineae)). Weedy volunteer vegetation include *Ageratum conyzoides* L. (Compositae), *Eupatorium odoratum* L. (Compositae), *Euphorbia hirta* L. (Euphorbiaceae), *Crassocephalum crepidioides* (Bth.) S. Moore (Compositae), *Imperata cylindrica* (L.) P. Beauv. var. *major* (Nees) C.E. Hubb. *ex* Hubb. & Vaugh. (Gramineae), *Melia aderazach* L. (Meliaceae), *Rorippa indica* (L.) Hiern (Cruciferae), *Saccharum spontaneum* L. (Gramineae), *Setaria palmifolia* (Korn.) Stapf var. *palmifolia* (Graminaea), *Solanum verbascifolium* L. (Solanaceae), and *Urena lobata* L. ssp. *lobata* var. *lobata* (Malvaceae). Bare ground is approximately 30–50%.

Abandoned field (AF): Short grasses, herbs, and shrubs occurring on abandoned fields or lands where grazing may limit tall vegetation growth. Species include *Helicteres angustifolia* L (Sterculiaceae), *Imperata cylindrica*, *Microstegium vagans* (Nees *ex* Steud.) A. Camus (Gramineae), *Miscanthus japonicus* (Thunb.) And. (Gramineae), *Paspalum conjugatum* Beerg. (Gramineae), *Rorippa indica*, *Saccharum spontaneum*, *Litsea cubeba* (Lour.) Pers. var. *cubeba* (Lauraceae), and *Mallotus albus* M.-A. (Euphorbiaceae).

Young secondary vegetation (YSV): Evergreen broadleaf bush mixed with *nua* (*Neohouzeoua dullooa* (Gamb.) A. Camus (Gramineae, Bambusoideae)) bamboo occurring in areas where forest was once cleared. Representative species include *Acacia pennata* (L.) Willd. (Leguminosae, Mimosoideae), *Cyperus nutans* Vahl (Cyperaceae), *Rauvolfia cambodiana* Pierre *ex* Pit. (Apocynaceae), *Eupatorium odoratum*, *Ficus* sp. (Moraceae), *Microstegium vagans*, *Saccharum spontaneum*, and *Urena lobata*.

Grassland (GL): Tall grasslands occurring where forest has been cleared and, perhaps, the land overworked during farming. Three species dominating this land cover, *Imperata cylindrica*, *Thysanolaena latifolia* (Roxb. *ex* Horn.) Honda (Gramineae)

and *Saccharum spontaneaum*, often reach heights exceeding 2–3 m and have extensive root systems that help them regenerate quickly after fire. Other common species are *Eupatorium odoratum*, *Microstegium vagans*, and *Urena lobata*.

Intermediate secondary vegetation (ISV): One-story 'forest' dominated by two bamboo species: *nua* and *giang* (*Ampelocalamus patellaris* (Gamb. Emend. Stap.) Stap. (Gramineae, Bambusoideae)). Other representative species include *Alpinia blepharocalyx* K. Sch. (Zingiberaceae), *Vernicia Montana* Lour. (Euphorbiaceae), *Cyperus nutans*, *Livistona saribus* (Lour.) Chev. (Palmae), *Pteris vittata* L. (Pteridaceae), and *Styrax tonkinensis* (Pierre) Pierre *ex* Guill. (Styracaceae). The understory is composed primarily of bamboo litter and shoots emerging from extensive root systems.

Forest (F): Disturbed evergreen broadleaf forest, attaining heights of 25–30 m. The discontinuous upper (25–30 m) and complex secondary (8–25 m) stories include the following representative tree species: *Heteropanax fragrans* (Roxb.) Seem. (Araliaceae), *Vernicia montana*, *Alphonsea tonkinensis A. DC.* (*Annonaceae*), *Melicope pteleifolia* (Champ. *ex* Bth.) T. Hart. (Rutaceae), *Garcinia planchonii* Pierre (Guttiferae), *Ostodes paniculata* Bl. (Euphorbiaceae), *Archidendron clypearia* (Jack) Niels. ssp. *clypearia* var. *clypearia* (Leguminosae, Mimosoideae), and *Schefflera heptaphylla* (L.) Frod. (Araliaceae). A bushy understory (2–8 m) and the forest floor includes *Breynia retusa* (Denn.) Alst. (Euphorbiaceae), *Bridelia hermandii* Gagnep. (Euphorbiaceae), *Cyperus nutans*, *Dioscorea depauperata* Prain & Burk. (Dioscoreaeceae), *Rauvolfia cambodiana*, *Ficus variegata* Bl. (Moraceae), *Livistona saribus*, *Miscanthus japonicus*, *Ostodes paniculata* Bl. (Euphorbiacaea), *Phrinium capitatum* Lour. (Marantaceae), *Psychotria rubra* (Lour.) Poir. (Rubiaceae), and *Selaginella monospora* Spring (Selaginelaceae).

References

Balmer, W.E., Williston, H.L., Dissmeyer, G.E., Pierce, C., 1982. Site preparation—why and how. Forest Manage. Bull. SA-FB2. USDA Forest Service, Atlanta, Georgia.

Barling, R.W., Moore, I.D., 1994. Role of buffer strips in management of waterway pollution: a review. Environ. Manage. 18, 53–558.

Bren, L.J., 2000. A case study in the use of threshold measures of hydrologic loading in the design of stream buffer strips. For. Ecol. Manage. 132, 243–257.

Brooks, R.H., Corey, A.T., 1964. Hydraulic properties of porous media. Hydrology paper 3. Colorado State University, Fort Collins, CO, p. 27.

Bruijnzeel, L.A., 2001. Forest hydrology. In: Evans, J.C. (Ed.), The Forests Handbook. Blackwell Scientific, Oxford, UK.

Castelle, A.J., Johnson, A.W., Conolly, C., 1994. Wetland and stream buffer size requirements: a review. J. Environ. Qual. 23 (5), 878–882.

Chalmers, R.W., 1979. Erosion from snig-tracks on granite/adamellite-derived soils. Aust. For. Res. Newsletter 6, 142.

Clinnick, P.F., 1985. Buffer strip management in forest operations: a review. Aust. For. 48 (1), 34–45.

Davies, P.E., Neilson, M., 1994. Relationships between riparian buffer widths and the effects of logging on stream habitat, invertebrate community composition, and fish abundance. Aust. J. Marine Freshwater Res. 45, 1289–1305.

De Ploey, J., Savat, J., Moeyersons, J., 1976. The differential impact of some soil factors on flow, runoff creep and rainwash. Earth Surf. Process. Landforms 1, 151–161.

Dillaha, T.A., Hayes, J.C., 1991. A procedure for the design of vegetative filter strips. Final Report to USDA Soil Conservation Service, Washington, DC, p. 48.

Dillaha, T.A., Reneau, R.B., Mostaghimi, S., Lee, D., 1989. Vegetative filter strips for agricultural nonpoint source pollution control. Trans. ASAE 32, 513–519.

Dosskey, M.G., Helmers, M.J., Eisenhauer, D.E., Franti, T.G., Hoagland, K.D., 2002. Assessment of concentrated flow through riparian buffers. J. Soil Water Conserv. 57 (6), 336–343.

Erman, D.C., Newbol, J.D., Roby, K.B., 1977. Evaluation of streamside bufferstrips for protecting aquatic organisms. Technical Completion Report No. 165, California Water Resources Center, CA.

Fahlen, A., 2002. Mixed tree-vegetative barrier designs: experiences from project works in northern Vietnam. Land Degrad. Dev. 13, 307–329.

Flanagan, D.C., Neibling, W.H., Foster, G.R., Hurt, J.P., 1986. Application of CREAMS in filter strip design. Paper No. 86-2043, ASAE, St. Joseph, USA.

Flanagan, D.C., Foster, G.R., Neibling, W.H., Burt, J.P., 1989. Simplified equations for filter strip design. Trans. ASAE 32, 2001–2007.

Fox, J., Dao Minh Truong, Rambo, A.T., Nghiem Phuong Tuyen, Le Trong Cuc, Leisz, S., 2000. Shifting cultivation: a new old paradigm for managing tropical forests. BioScience 50, 521–528.

Fox, J., Leisz, S., Dao Minh Truong, Rambo, A.T., Nghiem Phuong Tuyen, Le Trong Cuc, 2001. Shifting cultivation without deforestation: a case study in the mountains of northwestern Vietnam. In: Millington, A.C., Walsh, S.J., Osborne, P.E. (Eds.), Applications of GIS and Remote Sensing in Biogeography and Ecology. Kluwer Academic Publishers, Boston, pp. 289–307.

Garrity, D.P., Mercado Jr., A., Stark, M., 1998. Building the smallholder into successful natural resource management at the watershed scale. In: Penning de Vries, F.W.T., Angus, F., Kerr, J. (Eds.), Soil Erosion at Multiple Scales. CAB International, Wallingford, pp. 73–82.

Giambelluca, T.W., 2002. Hydrology of altered tropical forest. Hydrol. Process. 16, 1665–1669.

Gilliam, J.W., 1994. Riparian wetlands and water quality. J. Environ. Qual. 23, 896–900.

Gomi, T., Sidle, R.C., Richardson, J.S., 2002. Understanding processes and downstream linkages in headwater systems. BioScience 52, 905–916.

Graynoth, E., 1979. Effects of logging on stream environments and fauna in Nelson. N. Z. J. Marine Freshwater Res. 13, 79–109.

Haupt, H.F., 1959. A method for controlling sediment from logging roads. Intermountain Forest and Range Experiment Station Misc. Publ. no. 22.

Hayes, J.C., Dillaha, T.A., 1992. Vegetative filter strips application of design procedure. Paper No. 92-2103. American Society of Agricultural Engineers, St. Joseph, USA.

Herron, N.F., Hairsine, P.B., 1998. A scheme for evaluating the effectiveness of riparian zones in reducing overland flow to streams. Aust. J. Soil Res. 36, 683–698.

Hillel, D., 1971. Soil and Water—Physical Principles and Processes. Academic Press, NY.

Horton, R.E., 1919. Rainfall interception. Month. Weath. Rev. 47, 603–623.

Horton, R.E., 1933. The role of infiltration in the hydrologic cycle. Eos Trans. AGU 14, 446–460.

Jacinthe, P.-A., Groffman, P.M., Gold, A.J., Mosier, A., 1998. Patchiness in microbial nitrogen transformations in groundwater in a riparian forest. J. Environ. Qual. 27, 156–164.

Jordan, T.E., Correll, D.L., Weller, D.E., 1993. Nutrient interception by a riparian forest receiving inputs from cropland. J. Environ. Qual. 26 (3), 836–848.

Laurance, W.F., Bierregaard Jr., R.O., 1997. Preface: a crisis in the making. In: Laurance, W., Bierregaard, Jr., R.O. (Eds.), Tropical Forest Remnants: Ecology, Management, and Conservation of Fragmented Communities. University of Chicago Press, Chicago, IL, USA.

Le Trong Cuc, Rambo, A.T., 1999. Composite Swidden Farmers of Ban Tat: A Case Study of the Environmental and Social Conditions in a Tay Ethnic Minority Community in Hoa Binh Province, Vietnam. Research Report 1, Center for Natural Resources and Environmental Studies (CRES), Vietnam National University, Hanoi, 191 p.

Lee, K-H., Isenhart, T.M., Schultz, R.C., Mickelson, S.K., 2000. Multispecies riparian buffers trap sediment and nutrients during rainfall simulations. J. Environ. Qual. 29, 1200–1205.

Lee, P., Smith, C., Boutin, S., 2004. Quantitative review of riparian buffer width guidelines form Canada and the United States. J. Environ. Manage. 70, 165–180.

Lin, C.Y., Chou, W.C., Lin, W.T., 2002. Modeling the width and placement of riparian vegetated buffer strips: a case study on the Chi-Jia-Wang Stream Taiwan. J. Environ. Manage. 66, 269–280.

Lowrance, R., Dabney, S., Schultz, R., 2002. Improving water quality with conservation buffers. J. Soil Water Conserv. 57 (1), 36–43.

Lynch, J.A., Corbett, E.S., Mussallem, K., 1985. Best management practices for controlling nonpoint-source pollution on forested watersheds. J. Soil Water Conserv. 40 (1), 164–167.

Maag, M., Malinovsky, M., Nielsen, S.M., 1997. Kinetics and temperature dependence of potential denitrification in riparian soils. J. Environ. Qual. 26, 215–223.

Magette, W.L., Brinsfield, R.B., Palmer, R.E., Wood, J.D., 1989. Nutrient and sediment removal by vegetative filter strips. Trans. ASAE 32, 663–667.

Merz, B., Bardossy, A., 1998. Effects of spatial variability on the rainfall runoff process in a small loess catchment. J. Hydrol. 212–213, 304–317.

Meyer, L.D., Dabney, S.M., Harmon, W.C., 1995. Sediment-trapping effectiveness of stiff-grass hedges. Trans. ASAE 38, 809–815.

Morgan, R.P.C., 1995. Soil Erosion and Conservation. Longman Group Limited, Essex, UK, p. 198.

Munoz-Carpena, R., Parsons, J.E., Gilliam, J.W., 1999. Modeling hydrology and sediment transport in vegetative filter strips. J. Hydrol. 214, 111–129.

Norris, V., 1993. The use of buffer zones to protect water quality: a review. Water Resour. Manage. 7, 257–272.

O'Loughlin, E.M., 1981. Saturation regions in catchments and their topographic properties. J. Hydrol. 53, 229–246.

Parlange, J.-Y., Lisle, I., Braddock, R.D., Smith, R.E., 1982. The three-parameter infiltration equation. Soil Science 133 (6), 337–341.

Phillips, J.D., 1989. An evaluation of the factors determining the effectiveness of water quality buffer strips. J. Hydrol. 107, 133–145.

Plamondon, A.P., 1982. Increase of the concentration of sediments in a suspension according to forest use and length of the effect. Can. J. For. Res. 12 (4), 883–892.

Rambo, A.T., 1996. The composite swiddening agroecosystem of the Tay ethnic minority of the northwestern mountain of Vietnam. In: Rerkasem, B. (Ed.), Montane Mainland Southeast Asia in Transition. Chiang Mai University Consortium, Chiang Mai, Thailand, pp. 69–89.

Rawls, W.J., Brakensiek, D.L., Saxton, K.E., 1982. Estimation of soil water properties. Trans. ASAE 25 (5), 1316–1320 1328.

Schultz, R.C., Isenhart, T.M., Simpkins, W.W., Colletti, J.P., 2004. Riparian forest buffers in agroecosystems—lessons learned from the Bear Creek Watershed, Central Iowa, USA. Agroforestry Syst. 61, 35–50.

Sidle, R.C., Ziegler, A.D., Negishi, J.N., Abdul Rahim, N., Siew, R., Turkelboom, F. (2005) Erosion processes in steep terrain—truths, myths, and uncertainties related to forest management in SE Asia. Forest Ecol. Manage. (this issue).

Smith, C.M., 1992. Riparian afforestation effects on water yields and water quality in pasture catchments. J. Environ. Qual. 21, 237–245.

Smith, R.E., Goodrich, D.C., Quinton, J.N., 1995. Dynamic, distributed simulation of watershed erosion: the KINEROS2 and EUROSEM models. J. Soil Water Conserv. 50 (5), 517–520.

Smith, R.E., Goodrich, D.C., Unkrich, C.L., 1999. Simulation of selected events on the Catsop catchment by KINEROS2: A report for the GCTE conference on catchment scale erosion models. Catena 37, 457–475.

Srivastava, P., Costello, T.A., Edwards, R.R., Ferguson, J.A., 1998. Validating a vegetative filter strip performance model. Trans. ASAE 41 (1), 89–95.

Stephenson, G.R., Freeze, R.A., 1974. Mathematical simulation of subsurface flow contributions to snowmelt and runoff Reynolds Ck. Watershed Idaho. Water Resour. Res. 10, 284–294.

Tomer, M.D., James, D.E., Isenhart, T.M., 2003. Optimizing the placement of riparian practices in a watershed using terrain analysis. J. Soil Water Conserv. 58 (4), 198–206.

Trimble, G.R., Sartz, R.S., 1957. How far from a stream should a logging road be located? J. Forestry 55, 339–341.

van Groenewoud, 1977. Interim recommendation for the use of buffer strips for the protection of small streams in the Maritimes. Canadian Forest Service Information Report M-X-74, New Brunswick Department of Fisheries and Environment, Fredericton.

Vertessy, R., Elsenbeer, H., Bessard, Y., Lack, A., 2000. Storm runoff generation al La Cuenca. In: Grayson, R., Bloschl, G. (Eds.), Spatial Patterns in Catchment Hydrology: Observations and Modelling. Cambridge University Press.

Welsch, D.J., 1991. Riparian forest buffers. USDA-FS Publication no. NA-PR-07-91, USDA Forest Service, Radnor, PA.

Wischmeier, W.H., Smith, D.D., Predicting Rainfall Erosion Losses. Agriculture Handbook no. 53. USDA, Washington, DC, 1978.

Woolhiser, D.A., Smith, R.E., Goodrich, D.A., 1990. KINEROS, A Kinematic Runoff and Erosion Model: Documentation and User Manual. USDA-Agricultural Research Service, ARS-77, 130 p.

Wylie, R.E.J., 1975. Forest operation to safeguard water and soil resources. National Water and Soil Conservation Organization, Proceedings of Water and Soils Division, Course no. 2, Rotorua.

Ziegler, A.D., Sutherland, R.A., Giambelluca, T.W., 2000. Runoff generation and sediment transport on unpaved roads, paths, and agricultural land surfaces in northern Thailand. Earth Surf. Process. Landforms 25 (5), 519–534.

Ziegler, A.D., Sutherland, R.A., Giambelluca, T.W., 2001. Acceleration of Horton overland flow and erosion by footpaths in an agricultural watershed in Northern Thailand. Geomorphology 41 (4), 249–262.

Ziegler, A.D., Giambelluca, T.W., Tran, L.T., Vana, T.T., Nullet, M.A., Fox, J., Tran Duc Vien, Pinthong, J., Maxwell, J.F., Evett, S., 2004. Hydrological consequences of landscape fragmentation in mountainous northern Vietnam: Evidence of accelerated overland flow generation. J. Hydrol. 287, 124–146.